Journal of Power Sources 400 (2018) 256–263

Contents lists available at ScienceDirect

Journal of Power Sources

journal homepage: www.elsevier.com/locate/jpowsour

Remaining discharge-time prediction for batteries using the Lambert function

F. Quiñones[a,c,*], R.H. Milocco[a], S.G. Real[b]

[a] Grupo Control Automático y Sistemas (GCAyS), Departamento Electrotecnia, Facultad de Ingeniería, Universidad Nacional del Comahue, Buenos Aires, 1400, 8300 Neuquén, Argentina

[b] Instituto de Investigaciones Fisicoquímicas Teóricas y Aplicadas (INIFTA) Universidad Nacional de La Plata. Suc 4, CC16 (1900), La Plata, Argentina

[c] Universidad Tecnológica Nacional (UTN) Facultad Regional La Plata, La Plata, Argentina

HIGHLIGHTS

- The Lambert function is used to predict the remaining discharge-time in batteries.
- A simple electrochemical model is developed for batteries and compared with electrical circuits.
- The Lambert approach outperforms the electrical circuit runtime prediction.
- An upper bound of the error between both methods is obtained.
- A method to predict future demand is proposed.

ARTICLE INFO

Keywords:
Remaining discharge-time prediction
Electrochemical reduced-order model
Lambert function
Rate capacity effect
Electrical circuit model

ABSTRACT

The prediction of the remaining discharge-time in real-time is an important Battery Management System indicator in many engineering applications. It is the time in which the battery satisfies the load demanded until the voltage reaches its admissible lower limit. It is often obtained by the difference between the current and final charge scaled by a constant discharge current. The final charge can be obtained using a simple battery model like a pure integrator which leads to a simple but inaccurate solution. A more precise estimation is obtained by running models that take into account the Rate Capacity Effect but they are time consuming.

In this paper we propose to use the Lambert function for an accurate and fast prediction of the remaining discharge-time using a simple electrochemical model. We demonstrate that the errors in the prediction are similar to that obtained by running the well known electrical circuit. In order to illustrate the method, experimental parameter identification and remaining discharge-time predictions are carried out using a commercial Lithium-ion battery type.

1. Introduction

The Remaining Discharge-Time (RDT) is the period of time in which the battery, starting at a given initial condition, is able to satisfy the demand profile of current until the voltage reaches its admissible lower limit, E_{min}. Therefore, it becomes important for Battery Management Systems. The methods reported are based on the knowledge, in real-time, of the remaining discharge capacity which is proportional to the difference between present State of Charge, $SoC(0)$ and final $SoC(\Delta_t)$, where Δ_t is the RDT of the battery. For example the RDT of a battery with capacity Q for a constant discharge current of amplitude I is given by,

$$\Delta_t = \frac{Q}{I}(SoC(\Delta_t) - SoC(0)) \tag{1}$$

There are several and diverse reported methods to estimate $SoC(0)$. It can be obtained in real-time using model-based observers [1], Coulomb Counting [2], or the differential voltage analysis [3]. But, the case of predicting $SoC(\Delta_t)$ is more difficult because it depends on the discharge load profile and the dynamics of the battery. Methods for obtaining $SoC(\Delta_t)$ can be grouped in two sets, those based on model simulation and those obtained by characteristic maps.

A model-based approach consists in obtaining the states responses

* Corresponding author. Universidad Tecnológica Nacional (UTN), Facultad Regional La Plata, Av.60 esq. 124 , La Plata, Buenos Aires, Argentina. Tel.: +54 221 4257430; fax: +54 221 425 46442.

E-mail addresses: facundo.quinones@fain.uncoma.edu.ar (F. Quiñones), ruben.milocco@fain.uncoma.edu.ar (R.H. Milocco), sreal@inifta.unlp.edu.ar (S.G. Real).

https://doi.org/10.1016/j.jpowsour.2018.07.121
Received 23 July 2018; Accepted 30 July 2018
Available online 16 August 2018
0378-7753/ Published by Elsevier B.V.

by model simulation. Since the dynamics of a battery is governed primarily by mass diffusion processes, precise electrochemical models are computationally intensive. In order to avoid running the model, Rakhmatov and Virudhula [4], developed an analytical expression assuming planar diffusion processes of the electro-active species inside the battery. However, due to the complexity of the model, the solution of the equations must be approached using iterative methods. Thus, considering the limited computational power of the BMS, reducing the model order to a minimum becomes necessary. A widely used reduced-order model (ROM) is the electrical circuit. In case of known discharge current profiles, the predicted $SoC(\Delta_t)$ is obtained by simple simulation of the ROM, often called runtime prediction, until the voltage E_{min} is reached, [5]. For unknown current profiles, the same idea is used coupled with current predictions, [6]. Thus, the main drawback of obtaining the Predicted Remaining Discharge-Time (PRDT) by simulation in real-time is the computational cost and time consumption.

Other methods are based on considering the battery as a pure integrator and the errors are corrected by means of lookup tables. The advantage of using lookup tables is their simplicity but the prediction has poor accuracy because part of the battery internal dynamic is neglected. To improve the accuracy, several *adhoc* calibrations are proposed in [2], [3], [7].

In this paper, based on an electrochemical approach, we present a simple electrochemical model composed by the cascade of a pure integrator, a high pass-filter (HPF), and the Electromotive Force (EMF). All these components are related to explicit important electrochemical states like the SoC and the electrode surface charge concentration, which is a key variable for describing the concepts of the Rate Capacity Effect. Using this electrochemical model we present a closed solution for PRDT using the Lambert function.

The rest of the paper is organized as follows: in section 2 the electrochemical model is presented and their equations in terms of transfer function and state-space representation are obtained. In section 3, the explicit direct solution of PRDT for constant load profile using the Lambert function is presented. Using this approach, two different cases of discharge current are analysed: known constant current and unknown profile. In case of unknown profiles a prediction based on the moving averaged past values is proposed. In section 4 the model parameters identification using a periodic pulse of discharge current is developed. In section 5 the experimental results obtained with a commercial Lithium Ion (Li-ion) battery are used to illustrate the proposed method. Finally, in section 6, the conclusions are presented.

2. Electrochemical model

A battery is an electrochemical system composed of two electrodes immersed in an electrolytic media with an adequate porous separator. During discharge, the negative electrode is oxidized, while the positive electrode is reduced. The process is reversed during charge, being this global process responsible of the stored or released energy. At each electrode, the overall electrochemical processes involve a charge transfer reaction that takes place at the active material/electrolyte interface. This mechanism is coupled to the mass transfer process that could be occurring in the active material solid phase and/or the electrolyte.

The charge transfer process: The electrochemical reactions that take place at the electrochemical interface of the positive electrode (and simultaneously in the negative one) give rise to the battery current, I. Considering the kinetics follows a one-step reaction mechanism, and neglecting the capacitive currents related to the double layer, the current can be described by the Butler-Volmer equation as follows [8]:

$$I = k_r(1-X)\, e^{(1-\beta)\bar{\psi}\eta} - k_o X\, e^{-\beta\bar{\psi}\eta} \tag{2}$$

where $\eta = E^+ - E_{eq}$ is the positive electrode overpotential; E^+ is the voltage of the positive electrode and E_{eq} is the equilibrium constant voltage; $X \in (0,1)$ is the surface-fractional concentration with respect to the saturation of the reactant at the interface; k_r and k_o are constants that depends on the concentration of the reactants; $\bar{\psi}$ is a constant given by the quotient of the Faraday constant divided by the universal gas constant and the temperature and $\beta \in (0,1)$ is the symmetry factor.

The battery terminal voltage, E, is given by the difference of the electrode potentials and the voltage loss due to the internal resistance, r, as follows:

$$E = E^+ - E^- - Ir \tag{3}$$

$$E = \eta + E_{eq} - E^- - Ir \tag{4}$$

where E^- is the constant voltage of the non-limiting electrode. By replacing η from (4) in (2) the Butler-Volmer equation can be written as,

$$I = K_r(1-X)\, e^{\psi(E+Ir)} - K_o X\, e^{-\psi(E+Ir)} \tag{5}$$

Where $K_r = k_r\, e^{(E^- - E_{eq})}$; $K_o = k_o\, e^{-(E^- - E_{eq})}$ and at room temperature, $\psi = 19.7V^{-1}$. When $I = 0$, the terminal voltage becomes the Open Circuit Voltage (OCV) as follows:

$$K_r(1-X)\, e^{\psi\, OCV} = K_o X\, e^{-\psi\, OCV} \tag{6}$$

Taking logarithm on both sides of (6) the OCV is,

$$OCV = K_a + K_b \ln\left(\frac{X}{1-X}\right) \tag{7}$$

where $K_b = 1/2\psi$ and $K_a = K_b \ln(K_o/K_r)$. The relation described by (7) is called Electro-Motive Force, (EMF). Due to the relaxation of the system, in steady state, the electrode concentration X in both electrodes are homogeneous and equal to the SoC, therefore, the EMF can be obtained experimentally by measuring the OCV, in steady state, for different SoC levels.

On both electrodes there are secondary reactions that makes the EMF, although similar, not exactly the same as the ideal Butler-Volmer equation (7). Then, denoting the EMF generically as $f(X)$, the relationship between concentration, current, and terminal voltage of the battery, denoted here by $F(X, E, I)$, has the following expression:

$$F(X, E, I) = E - f(X) + Ir = 0 \tag{8}$$

The mass transfer process: The concentration X is determined by the dynamics of the mass transport, essentially diffusional processes of the reactants either in the electrolyte or in the electrode active materials. The diffusional processes governed by Fick's laws constitute the second part of the model. The transport processe is a distributed parameter system formulated in terms of the Laplace Transform with the following general expression:

$$\mathbb{X}(S) = \mathbb{D}(S)\mathbb{I}(S) \tag{9}$$

where S is the Laplace complex variable; $\mathbb{D}(S)$ is the Laplace Transform of the diffusional process; and $\mathbb{X}(S)$ and $\mathbb{I}(S)$ are the Laplace Transform of $X(t)$ and $I(t)$, respectively. In Ref. [9], the expression of $\mathbb{D}(S)$ for finite diffusion in planar, cylindrical and spherical geometry with a Nernstian or impermeable diffusion layer boundary conditions is obtained. Multiplying and dividing by SQ in (9) the diffusional process can be written as a product of a pure integrator and the impedance $G(s)$ as follows:

$$\mathbb{X}(S) = G(S)\mathbb{SOC}(S) \tag{10}$$

$$\mathbb{SOC}(S) = \mathbb{I}(S)/SQ \tag{11}$$

where, $G(S) = \mathbb{D}(S)SQ$ and $\mathbb{SOC}(S)$ is the Laplace Transform of $SoC(t)$. In Ref. [10] it is shown that $G(S)$ is a HPF with unitary steady-state gain and model the Rate Capacity Effect (RCE) of the battery. The RCE is the phenomenon of the battery by which the capacity depends on the charge/discharge profile. Great charge demands reduces excessively the voltage. In Ref. [9], the transfer function $G(S)$ for the planar, cylindrical and spherical electrode particle geometries were devised and they are depicted in Table 1.

Table 1
The analytical expressions of $G(S)$ for different geometries, where $\phi = \sqrt{S\Gamma}$, Γ is the time constant diffusion also known as the characteristic length of the electrode; where I^0 and I^1 are the first kind modified Bessel functions of zero and first order.

Planar	Spherical	Cylindrical
$G(S) = \phi\coth\phi$,	$G(S) = \frac{\phi^2}{3}\frac{\tanh\phi}{(\tanh\phi - \phi)}$	$G(S) = \frac{\phi I^0(\phi)}{I^1(\phi)}$

Models as those depicted in Table 1, are infinite dimensional and cannot be used for real-time applications, instead ROMs are used. We consider a unitary gain first order pole-zero approximations of RCE, named $G^1(S)$ as follows:

$$G^1(S) = \frac{aS + 1}{ps + 1};\ 0 < p < a \tag{12}$$

We use the notation $G^0 = 1$ for ideal batteries modelled as a pure integrator without RCE. In order to compare the performance of the reduced-order approximation respect to the full order model listed in Table 1, the energy of the difference between the concentration X of the full order model and the corresponding of the ROM is computed. The square root of this energy is the RMSE of the difference and can be obtained in frequency domain using the Parseval Theorem. Using equation (10), the RMSE of the difference between full and reducer order approximation of X is given by:

$$RMSE = \left[\int_{-\infty}^{\infty} |(G(j\omega) - G^i(j\omega))|^2 |\$\mathbf{O}\mathbb{C}(j\omega))|^2 d\omega\right]^{1/2} \tag{13}$$

The substitution $S = j\omega$ in equation (10) was used to obtain the expressions in frequency domain. Using a pulse load of current as in Fig. 1 and $G(S)$ from Table 1, the RMSE for spherical and planar diffusions as a function of the pulse duration, T, is shown in Fig. 2 for $i = 0$ and $i = 1$. Instead of pulse duration, in these figures we use the C-Rate. The C-Rate (C/T) means that a completely charged battery is entirely discharged in T-hours. Adopting a typical value of the time constant diffusion of $G(S)$, $\Gamma = 37.5s^{-1}$, the parameters a and p of the $G^1(S)$ are optimized for each value of the C-Rate in the range [0.1–10]C in order to obtain the lower bound, named G^1_{LB} in Fig. 2, of the RMSE. The error when the parameters are identified using pulses of 0.1C, denoted as $G^1_{0.1}$, and 1C, denoted as G^1_1, are also depicted in Fig. 2 in order to show that the error performs very close to the lower bound no matter the specific value of C-rate of the pulse. It can also be observed that the first order approximation reduces the error significantly with respect to the zero order approximation, $G^0 = 1$ and the error becomes zero when C-Rate is lesser than one.

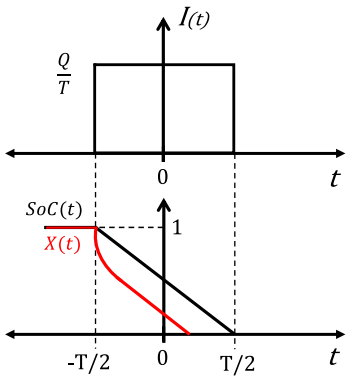

Fig. 1. Pulse of current and diffusional time-response.

2.1. Step response of the reduced-order electrochemical model

The complete model of the battery is formed by the cascade of the pure integrator, with gain $-1/Q$, the high pass filter representing the RCE and the charge transfer equation (8). A schematic representation of the electrochemical model is depicted in Fig. 3. The reduced order electrochemical model (ECHM) is obtained using $G^1(S)$. From this ECHM, the time step response of a current with amplitude I, for $t > 0$, is given in matrix time-domain formulation as follows:

$$\zeta_q(t) = A_q(t)\zeta_q(0) + B_q(t)I \tag{14}$$

$$E_q(t) = f(X(t)) - Ir_q \tag{15}$$

where $\zeta_q(t) = \begin{bmatrix} SoC(t) \\ X(t) \end{bmatrix}$; $A_q(t) = \begin{bmatrix} 1 & 0 \\ 1 - e^{-t/p} & e^{-t/p} \end{bmatrix}$; $B_q(t)$;

$$= \begin{bmatrix} -t \\ (p-a)(1 - e^{-t/p}) - t \end{bmatrix}\frac{1}{Q}$$

This expression will be useful for the determination of the remaining time in next section.

3. PRDT using the ECHM

Given arbitrary initial values of the SoC and X at time t we distinguish two different scenarios for the PRDT, 1) Constant-current load and 2) Unknown future piecewise load.

3.1. PRDT for constant-current

Assuming a constant load of amplitude I, starting at time $t = 0$, the concentration X at time Δ_t is obtained from (14) as,

$$X(\Delta_t) = \left(1 - e^{-\Delta_t/p}\right)SoC(0) + e^{-\Delta_t/p}X(0) + \left((p-a)\left(1 - e^{-\Delta_t/p}\right) - \Delta_t\right)\frac{I}{Q} \tag{16}$$

it can be written in a compact form as

$$\Delta_t + \rho_1 + e^{-\Delta_t/p}\rho_2 = 0 \tag{17}$$

Where ρ_1 and ρ_2 are given by:

$$\rho_1 = (X(\Delta_t) - SoC(0))\frac{Q}{I} - (p - a) \tag{18}$$

$$\rho_2 = (SoC(0) - X(0))\frac{Q}{I} + (p - a) \tag{19}$$

Both ρ_1 and ρ_2 are known quantities that depend on the initial conditions and $X(\Delta_t)$ is a priori known using (15),

$$X(\Delta_t) = f^{-1}(E_{min} + Ir_q) \tag{20}$$

Multiplying by $(1/p)e^{(\Delta_t + \rho_1)/p}$ both sides of (17) yields

$$we^w = y \tag{21}$$

where $w = (\Delta_t + \rho_1)/p$ and $y = -(\rho_2/p)e^{\rho_1/p}$. The value of w is obtained solving equation (21) using the Lambert function $w = \mathbf{w}[y]$, [11]. Finally, the RDT is obtained at any time by,

$$\Delta_t = w\,p - \rho_1 \tag{22}$$

Although the Lambert function, has not an explicit expression, it can be well approximated using closed expressions or accessed via lookup table (see figure in the supplementary material).

Remark 1. In case of an ideal battery, $G^0 = 1$, $a = p$ and the system fulfils $SoC = X$. Thus, $\rho_2 = 0$, $w = 0$, $SoC(\Delta_t) = X(\Delta_t) = 0$, and the RDT gives, as expected:

$$\Delta_t = -\rho_1 = \frac{SoC(0)Q}{I} \tag{23}$$

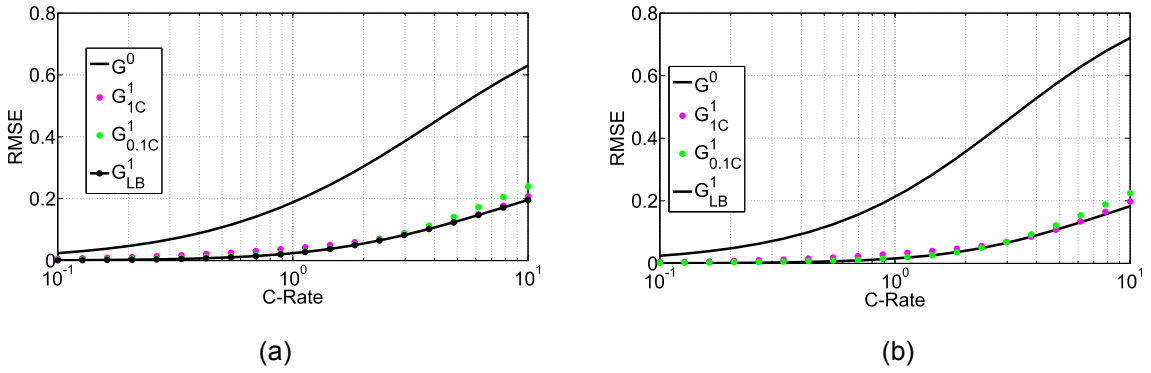

Fig. 2. Performance evaluation of zero, $G^0(S)$, and first, $G^1(S)$ order approximations of RCE, $G(S)$, for a) spherical diffusion and b) planar diffusion.

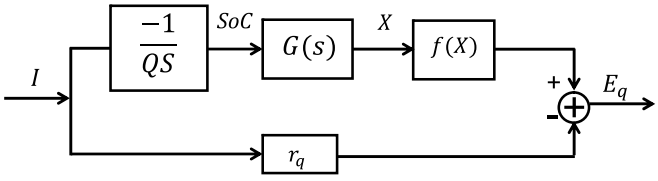

Fig. 3. Schematic representation of the electrochemical model.

This is often called *SoC*-based method for PRDT.

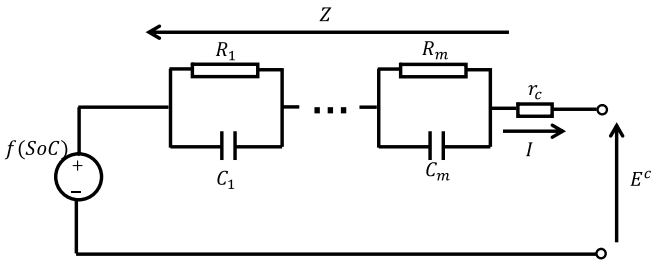

Fig. 4. Electrical circuit model.

3.2. PRDT for unknown future piecewise load

In cases where the future load is unknown, based on the past data, it is possible to predict an equivalent more probable constant-current that will discharge the battery. Then, the PRDT is obtained using equation (22) with the equivalent constant discharge load $\bar{I}$. This current can be recursively obtained at each step k as a mean value of the historical data as follows:

$$\bar{I}(k) = \frac{\sum_{i=1}^{k} \lambda^{k-i} I(i)}{\sum_{i=1}^{k} \lambda^{k-i}} \tag{24}$$

where λ is an scalar in the interval (0,1] called the *forgetting factor*. It performs an exponential windowing over the previous current amplitudes depending on the value of λ. If $\lambda < 1$, previous prediction contributes only marginally to the present estimation of $\bar{I}(k)$. The window's width is reduced as λ decreases. In case of $\lambda = 1$, all past data are equally weighted and the classical averaged value is obtained. Thus, the value of λ determines the memory of the past data, which is a suitable parameter to take into account for time-variant mobility dynamics. A recursive formulation for numerator $n(k)$ and denominator $d(k)$ of equation (24) is convenient to reduce the computational cost as follows:

$$n(k) = \sum_{i=1}^{k} \lambda^{k-i} I(i) = I(k) + \lambda \sum_{i=1}^{k-1} \lambda^{k-i-1} I(i) = I(k) + \lambda n(k-1); \quad k \geq 1 \tag{25}$$

$$d(k) = \sum_{i=1}^{k} \lambda^{k-i} = 1 + \lambda \sum_{i=1}^{k-1} \lambda^{k-i-1} = 1 + \lambda d(k-1); \quad k \geq 1 \tag{26}$$

Finally, given initial values $n(0) = I(0)$ and $d(0) = 1$ the time-variant mean value at each k estimated over the exponentially-weighed past samples is:

$$\bar{I}(k) = \frac{I(k) + \lambda n(k-1)}{1 + \lambda d(k-1)} \tag{27}$$

4. Electrical circuit model

For comparison performances we use the electrical circuit model depicted in Fig. 4. The impedance of the *RC*-parallel circuits represents the RCE and it is obtained using the voltage loss $Z(t)$, with Laplace Transform $\mathbb{Z}(S)$. The first order approximation of the impedance has the following expression:

$$\frac{\mathbb{Z}(S)}{\mathbb{I}(S)} = H(S) = \frac{R}{1 + RCS} \tag{28}$$

Using the Laplace Antitransform of equation (28), the time response of the reduced-order electrical circuit model (ECM) to a current step of constant amplitude I for $t > 0$ is given in matrix time-domain formulation as follows:

$$\zeta_c(t) = A_c(t)\zeta_c(0) + B_c(t)I \tag{29}$$

$$E_c(t) = f(SoC(t)) - Z(t) - Ir_c \tag{30}$$

where

$$\zeta_c(t) = \begin{bmatrix} SoC(t) \\ Z(t) \end{bmatrix}; \; A_c(t) = \begin{bmatrix} 1 & 0 \\ 0 & e^{-t/RC} \end{bmatrix}; \; B_c(t) = \begin{bmatrix} -t/Q \\ R(1 - e^{-t/RC}) \end{bmatrix};$$

Different from the case of the ECHM, the state variables *SoC* and *Z* of the ECM are decoupled, thereby, PRDT requires the knowledge of $SoC(\Delta_t)$ which is impossible to obtain explicitly. Then, for the ECM is not possible to obtain a direct PRDT calculation. Instead, recursive numerical methods or discrete-time model simulations are needed.

Assuming the load-current is represented by a piecewise constant load $I(t)$ during constant periods of time h_s as it is shown in Fig. 5 and using equations 29 and 30 the discrete-time response at sampling time $t = (k+1)h_s$, where k is an integer, is given by the initial conditions of the states at $t = kh_s$ as follows:

$$\zeta_c(k+1) = A_c\zeta_c(k) + B_cI(k) \tag{31}$$

$$E_c(k) = f(SoC(k)) - Z(k) - I(k)r_c \tag{32}$$

where kh_s was replaced for k for simplicity, $A_c = A_c(h_s)$ and $B_c = B_c(h_s)$ are a matrix and a vector of constants. A working algorithm to obtain the RDT, starting at present known values of $SoC(k)$ and $Z(k)$, consists

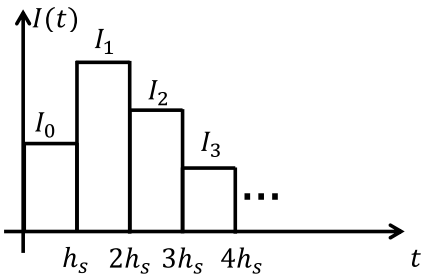

Fig. 5. Arbitrary constant piecewise current, at constant intervals of h_s duration.

of iterating equation (31) until the voltage of equation (32) reaches its minimum admissible value, $E_c(k+M) \leq E_{min}$. The PRDT is an integer, M, such as $(M-1)h_s < \Delta_t \leq Mh_s$. Note that the accuracy increases as h_s becomes smaller. The main advantage of this discrete-time approach is the simplicity and straightforward implementation. However, this method has a large consumption of time and computational cost due to the simulation between samples.

Remark 2. In case of *EMF* was a linear function, say $f(X) = \alpha X$ for ECHM or $f(SoC) = \alpha SoC$ for ECM, where α is a constant, both models ECHM and ECM are equivalents under the following equalities $SH(S)Q = \alpha(G^1(S) - 1)$, and $Z = \alpha(SoC - X)$. However, the *EMF* is a nonlinear function and will lead to differences in the PRDT depending on which model is used.

Remark 3. In the Appendix, a formal proof of the upper bound for the differences between the PRDT obtained by ECHM and by ECM is given. In short it is,

$$\left|\Delta_{tc} - \Delta_{tq}\right| \leq C_B; \text{ where } C_B = \frac{\gamma}{|f'(\Delta_t)|}\frac{Q}{I} \tag{33}$$

Where Δ_{tc} is the PRDT of ECM using the discrete-time model simulation described above and Δ_{tq} is the PRDT of ECHM calculated using equation (22); γ is a bound given by the absolute maximum of the voltage difference between both models; and $f'(\Delta_t) = \partial f/\partial SoC$ is the partial derivative of the *EMF* with respect to the *SoC* evaluated at true RDT, Δ_t. For example using the reasonable value of $f'(\Delta_t) = 2$ and supposing that the voltage difference between both models is bounded by $\gamma = 0.02$ V, the upper bound of the difference between both PRDT, for 1C, is lower than $0.01h$. In summary, the difference between the PRDT using both models is proportional to the upper bound of the voltage difference of both models.

5. Experimental results

The first step is the identification of the *EMF* and the capacity Q of the battery. After obtaining these results we proceed to the identification of parameters a, p and r_q of the ECHM, and R, C and r_c of the ECM according to the following procedure: with the battery fully charged at E_0 voltage, intermittent pulses of current are applied until the battery is fully discharged reaching the steady voltage E_{end} as depicted in Fig. 6(a). We call this periodic pulses of current, $I_\Delta(t)$. The period is N T , where T is the duration of each pulse and N is the number of pulse intervals until the transient of the RCE vanishes. The capacity is obtained by adding all the charge decrements, $DQ = I \times T$ from battery fully charged to fully discharged. Since at the end of each period the *SoC* is equal to X, the *EMF* is obtained by measuring the *OCV* and computing the *SoC* by Coulombing Counting. The number of samples obtained for the *EMF* is equal to the amount of pulses used to discharge the battery. The discrete values of *SoC* depends on the amount of charge that each pulse extracts. We consider equal pulse amplitudes for simplicity but they can be different. All these operations are made by using discrete-time sampled values of $I_\Delta(t)$ at $t = kh_s$ for $k = 1, ..., K$, where Kh_s is the final time of the load profile.

We will show experimental results at room temperature on a commercial lithium battery *Samsung (EB-BG900BBC)* with nominal capacity $Q_{nom} = 2.8Ah$, and nominal voltage $3.8V$. Starting in steady state with $SoC = 0.98$ and $E_0 = 4.4V$, regular intermittent 55 discharge current pulses of $0.15A$ amplitude, each during $T = 0.25h$, were applied until $SoC = 0.12$ and voltage equal to $3.4V$ was reached. The rest time between discharge pulses was $1.75h$ ($N = 7$ times T), see Fig. 6(b). The sampling period was $h_s = 20s$ and the total experiment takes $K \times h_s = 110h$. The identified capacity was $Q = 2.7Ah$ and the *EMF* is shown in Fig. 6(d).

The parameters a, p and r_q of the ECHM and R, C and r_c of the ECM are identified using the same load profile $I_\Delta(t)$ with the *EMF* and Q obtained before. The model parameters are obtained by minimizing the Mean Squared Error, *MSE*, given by equation (34). The terminal voltage error, $\varepsilon(k)$, $k = 1, ..., K$, is the difference between the measured and the model-voltage valued at every $t = k\,h_s$. The identification procedure was made using the standard optimization algorithm Simplex.

$$MSE = \sum_{k=1}^{K} \left|\varepsilon(k)\right|^2 \tag{34}$$

In Fig. 6(c) the measured voltage and the ones obtained from the numerical minimization from both models are shown. The identified values are listed in Table 2.

Using the two identified models, we will evaluate the errors between PRDT through the Lambert solution in the ECHM and by running a simulation of the ECM as described in section 4 for constant current profile. For this purpose we use a set of six experiments of several charge and discharge cycles each with constant current of random amplitudes (see figure in the supplementary material). In all the experiments, the battery was discharged until the voltage $E_{min} = 3.43V$ was reached. From this experimental set we obtain the real RDT values, $\Delta_t(i)$, and the PRDT $\Delta_{tq}(i)$ and $\Delta_{tc}(i)$ for both the ECHM and ECM respectively, for $i = 1$ to 33. In the six experiments, the battery was started from its steady state condition. The initial condition of the state variables was obtained using the *EMF*. Thus, the states at actual time are known by running recursively equations 31 and 32 for the ECM and (14)–(15) for the ECHM. Using the values of the states at each k, the PRDT is obtained using equation (22) for the ECHM and by running the discrete-model equations 31 and 32 for the ECM until the voltage-model fulfils the condition $E_c(k+M) \leq E_{min}$.

It must be noticed that for the case of ECM, the total error when running the model is the sum of the modelling error plus the discretization error that depends on the selected sampling period h_s as described in section 4. Thus, large sampling periods means fewer number of recursions but large uncertainty error and viceversa. Contrary to the ECM, the predictions using the Lambert approach is not affected by the sampling error.

In Fig. 7, the PRDT errors obtained from the six experiments by using the Lambert function versus the error by running the ECM are depicted. In Fig. 7(a) the sampling period used was $h_s = 10s$. The black line represents the case where both error are equal, $\Delta_{tq} = \Delta_{tc}$. The red line is the linear regression fitted using the error data set where the slope lesser than one indicates a better performance of the Lambert approach with respect to ECM recursions. In the figures, the bound of the difference between both estimations obtained by equation (33) is also depicted. In Fig. 7(b) the same is shown but in this case using $h_s = 60s$.

To evaluate the performance in the case of predicting the future current, a new load profile was tested. In Fig. 8(a) the current profile and the predicted mean value using equations 25–27 with $\lambda = 0.985$, $\lambda = 0.99$ and $\lambda = 1$ are shown. The PRDT using equation (22) with the current $\bar{I}$ calculate for each value of λ are shown in Fig. 8(b). It can be

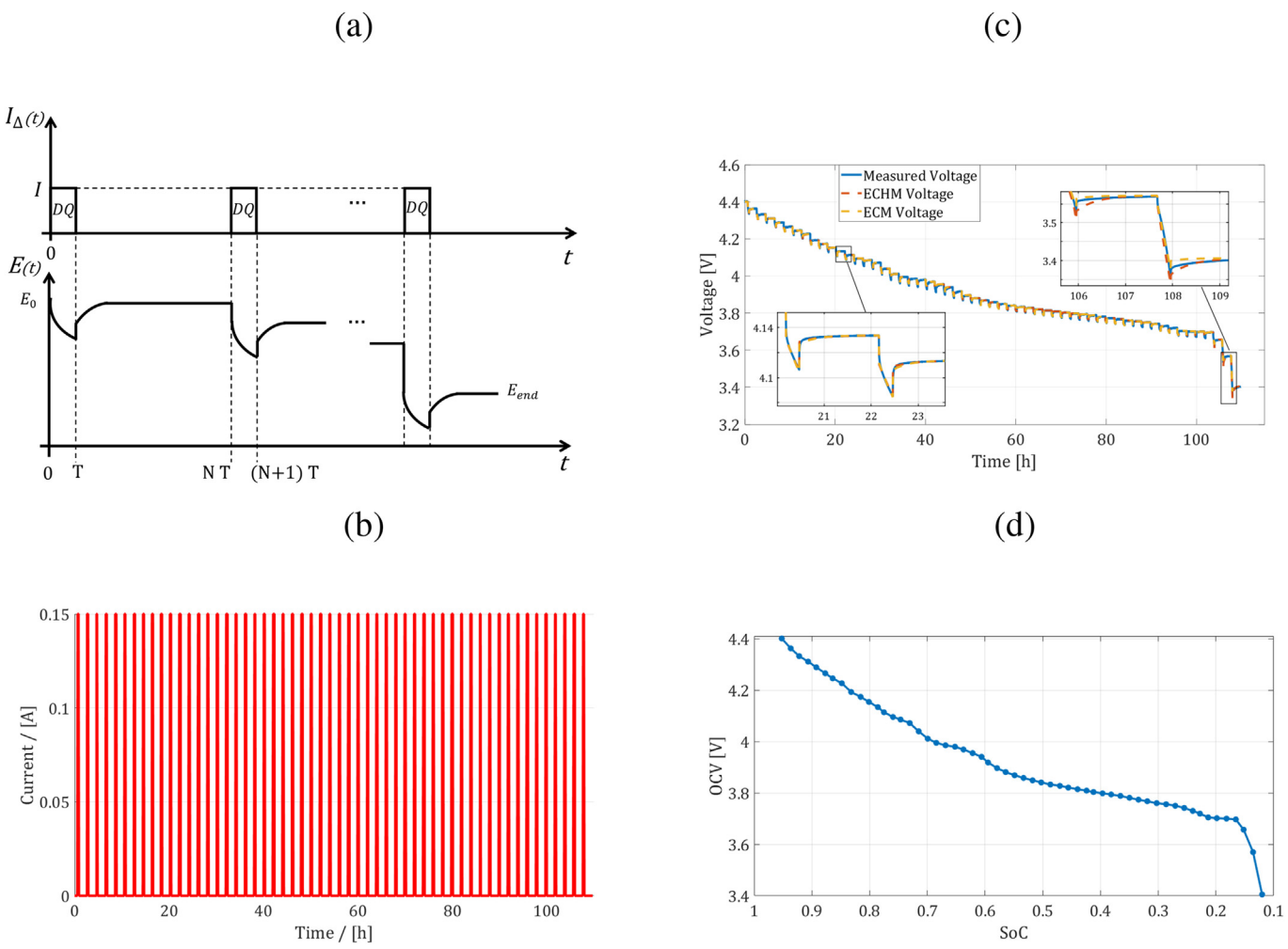

Fig. 6. (a) Schematic test signal $I_\Delta(t)$ formed by periodic pulses of current with small area. (b) $I_\Delta(t)$ signal of current applied to a commercial Li-ion battery in order to identify the parameters of the ROMs. (c) Battery and ECHM and ECM voltage responses to $I_\Delta(t)$ signal. (d) EMF curve obtained through $I_\Delta(t)$ test.

Table 2
Optimal parameters obtained by minimizing the MSE of the voltage error using the $I_\Delta(t)$ profile.

ECHM	ECM
$a = 0.591\ h^{-1}$	$R = 0.085\ \Omega$
$p = 0.436\ h^{-1}$	$C = 13900\ F$
$r_q = 0.152\ \Omega$	$r_c = 0.144\ \Omega$

seen that it is possible to calculate the PRDT with an appropriate value of λ, using the Lambert equation considering $\bar{I}$ instead of I.

6. Conclusions

The remaining discharge-time prediction using the Lambert function together with an electrochemical reduced-order model for rechargeable batteries was presented. Two possible load discharge scenarios were analysed: the known constant discharge current and the unknown future discharge current. The predictions obtained were statistically evaluated showing bounded errors for different prediction horizons. The proposed method has been compared to the well-known procedure of estimating the remaining discharge-time by running in real-time a reduced-order electrical circuit model. It was analytically demonstrate and experimentally tested that the two models have a similar performance with small bounded errors. However, using the Lambert function, the latency time and the energy consumption of the electrical circuit model approach are avoided.

Acknowledgments

This work was supported by the Consejo Nacional de Investigaciones Científicas y Técnicas (CONICET), Agencia Nacional de Promoción Científica y Técnica, Universidad Nacional del Comahue, Universidad Nacional de La Plata, Universidad Tecnológica Nacional Facultad Regional La Plata; all in República Argentina.

Appendix

The error between the true and ECM voltage, for constant current I, at time Δ_t is,

$$E_{min} - E_c(\Delta_t) = E_{min} - f(SoC(\Delta_t)) + Z(\Delta_t) + Ir_c = \varepsilon_c(\Delta_t) \tag{35}$$

and at time Δ_{tc} is,

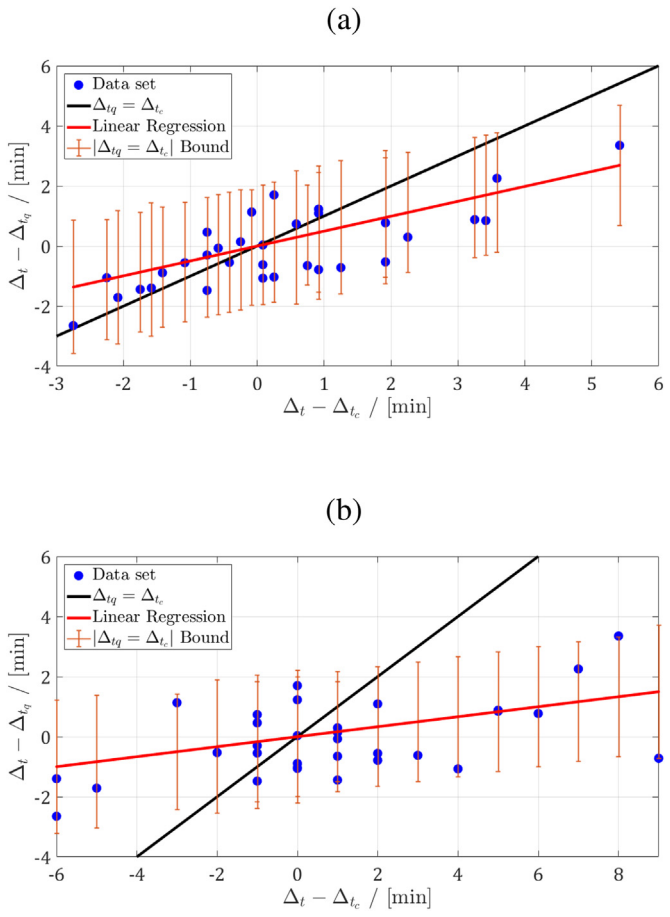

Fig. 7. Blue: Lambert versus running-time PRDT error data set. Black: $\Delta_{tq} = \Delta_{tc}$ line; Red: linear regression of data; Orange: error bound; (a) $h_s = 10s$. (b). (For interpretation of the references to colour in this figure legend, the reader is referred to the Web version of this article.)$h_s = 60s$.

$$E_{min} - E_c(\Delta_{tc}) = E_{min} - f(SoC(\Delta_{tc})) + Z(\Delta_{tc}) + Ir_c = 0 \tag{36}$$

By substracting (36) to (35) we obtain,

$$[f(SoC(\Delta_{tc})) - f(SoC(\Delta_t))] - [Z(\Delta_{tc}) - Z(\Delta_t)] = \varepsilon_c(\Delta_t) \tag{37}$$

Assuming that Δ_t is close to Δ_{tc} the left side of the equation can be approximated by the first term of the Taylor series expansion around time Δ_t as follows:

$$\varepsilon_c(\Delta_t) \approx (f'_s SoC' - Z')(\Delta_t)(\Delta_{tc} - \Delta_t) \tag{38}$$

where $f' = \partial f/\partial SoC$, $SoC' = \partial SoC/\partial t$ and $Z' = \partial Z/\partial t$ are partial derivatives evaluated at $t = \Delta_t$.

Using a similar reasoning for ECHM at time $t = \Delta_{tq}$, the following holds:

$$\varepsilon_q(\Delta_t) \approx (f'X')(\Delta_t)(\Delta_{tq} - \Delta_t) \tag{39}$$

where $f' = \partial f/\partial SoC = \partial f/\partial X$ and $X' = \partial X/\partial t$. Taking into account the linear approximation around $t = \Delta_t$ and using Remark 2, both models are

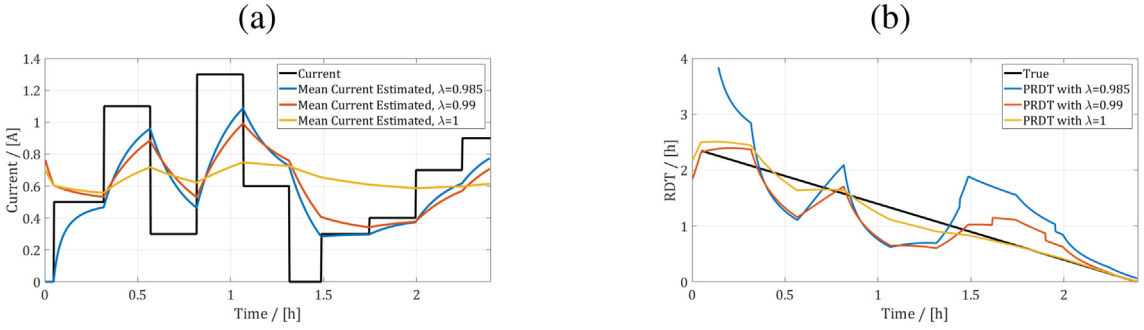

Fig. 8. (a) Unknown load profile and online estimated mean current for different values of λ. (b) PRDT using the Lambert function for different values of λ.

locally equivalents and $f'SoC' - Z' \approx f'X'$ holds.Thereby, by subtracting (39) from (38) and taking absolute value we obtain the bound of the difference between both PRDT as follows:

$$\left|\Delta_{tc} - \Delta_{tq}\right| \approx \frac{|\varepsilon_c(\Delta_t) - \varepsilon_q(\Delta_t)|}{|(f'X')(\Delta_t)|} \tag{40}$$

$$\leq \frac{\gamma}{|(f'X')(\Delta_T)|} \tag{41}$$

$$\leq \frac{\gamma}{|(f'SoC')(\Delta_t)|} = \frac{\gamma}{|f'(\Delta_t)|}\frac{Q}{I} \tag{42}$$

where γ is the upper bound of voltage error $|E_c(t) - E_q(t)|, \forall\, t$. The inequality (42) was obtained using the fact that $SoC' = I/Q$ for constant discharge current and $|X'|$ is greater than or equal to $|SoC'|, \forall\, t$, see Fig. 1.

Appendix A. Supplementary data

Supplementary data related to this article can be found at https://doi.org/10.1016/j.jpowsour.2018.07.121

References

[1] W. Waag, C. Fleischer, D.U. Sauer, Critical review of the methods for monitoring of lithium-ion batteries in electric and hybrid vehicles, J. Power Sources 258 (2014) 321–339.

[2] V. Pop, H.J. Bergveld, P.H.L. Notten, J.H.G. Op het Veld, P.P.L. Regtien, Accuracy analysis of the State-of-Charge and remaining run-time determination for lithium-ion batteries, Measurement 42 (2009) 1131–1138.

[3] G. Liu, M. Ouyang, L. Lu, Jianqiu Li, X. Han, Online estimation of lithium-ion battery remaining discharge capacity through differential voltage analysis, J. Power Sources 274 (2015) 971–989.

[4] D.N. Rakhmatov, S. Vrudhula, An analytical high-level battery model for use in energy management of portable electronic systems, Proc. IEEE/ACM Int. Conf. Comput. Aided Design (2001) 488–493.

[5] M. Chen, G. Rincon-Mora, Accurate electrical battery model capable of predicting runtime and I-V performance, IEEE Trans. Energy Convers. 21 (2006) 504–511.

[6] Guangzhong Dong, Jingwen Wei, Zonghai Chen, Sun Han, Xiaowei Yu, Remaining dischargeable time prediction for lithium-ion batteries using unscented Kalman filter, J. Power Sources 346 (2017) 316–327.

[7] D. Doerffel, S.A. Sharkh, A critical review of using the Peukert equation for determining the remaining capacity of lead-acid and lithium-ion batteries, J. Power Sources 155 (2006) 395–400.

[8] J.O.'M. Bockris, A.K.N. Reddy, M. Gamboa-Aldeco, Modern Electrochemistry 2A. Fundamentals of Electrodics, second ed., Kluwer Academic Plenum Publishers, 2000.

[9] T. Jacobsen, K. West, Electrochim. Acta 40 (No2) (1995) 255–262.

[10] R.H. Milocco, J.E. Thomas, B.E. Castro, Generic dynamic model of rechargeable batteries, J. Power Sources 246 (2014) 609–620.

[11] R.M. Corless, G.H. Gonnet, D.E.G. Hare, D.J. Jeffrey, D.E. Knuth, On the Lambert W function, Advances in Computational Maths 5 (1996) 329–359.